Electronic Supplementary Material (ESI) for RSC Advances.

Localized Surface Plasmon Resonance Shift of Biosynthesized and Functionalized Quasi-Spherical Gold Nanoparticle Systems

Ricky Kristan M. Raguindin and Candy C. Mercado

Supplementary Information

Figures

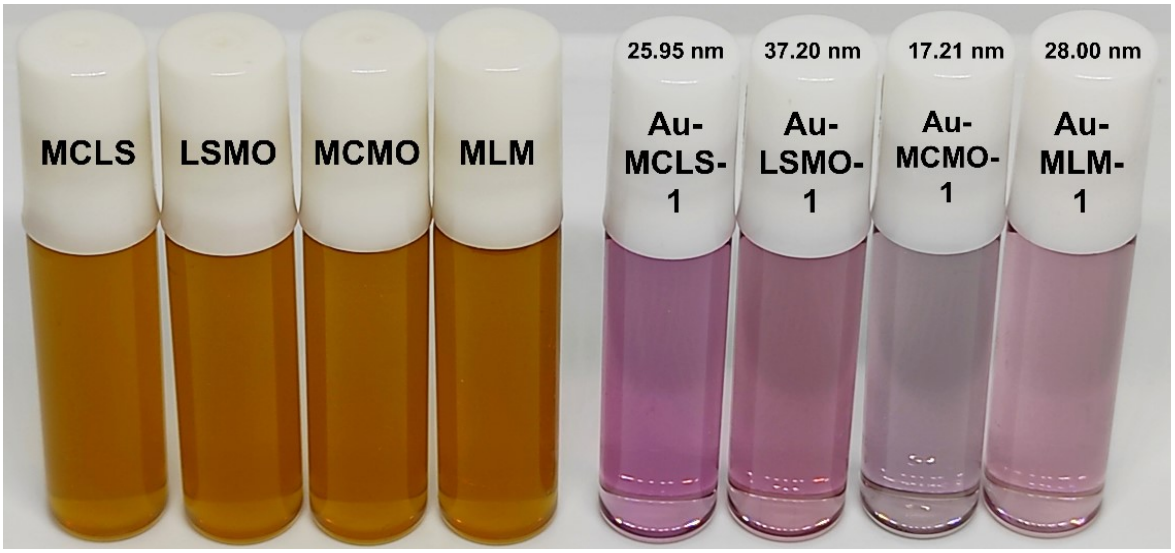

Figure S1 Comparison of the colors of combined leaf extracts and their corresponding biosynthesized Au-nanoparticle systems.

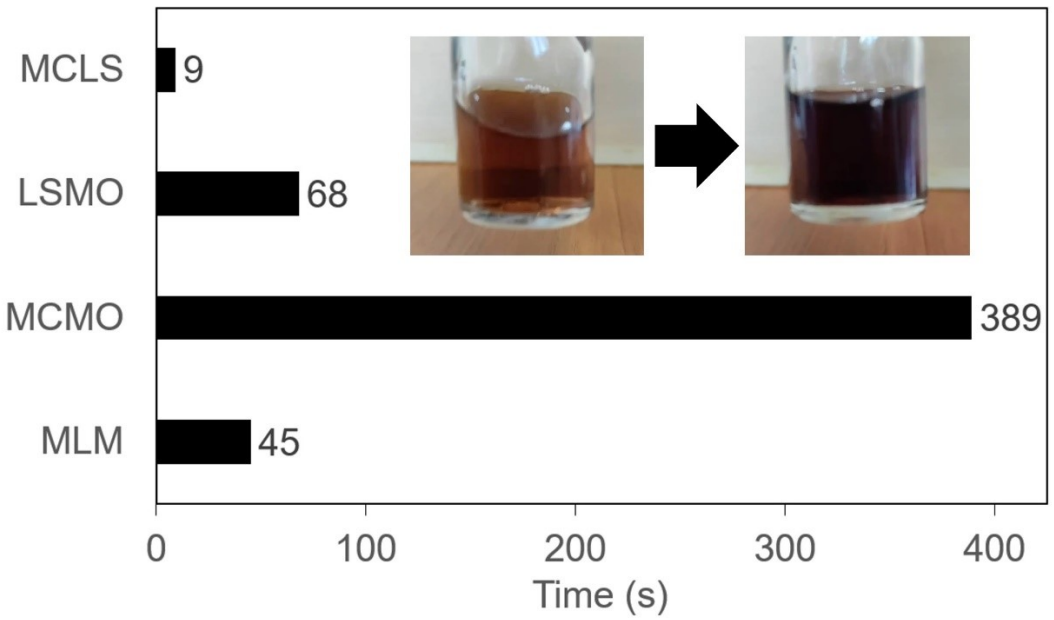

Figure S2 Comparison of time for Au nanoparticle formation at room temperature using different combined leaf extracts. In general, the endpoint for time recording was signalled by a color change (inset) from amber brown (extract) to brownish deep violet/purple (unpurified system of Au nanoparticles with extract).

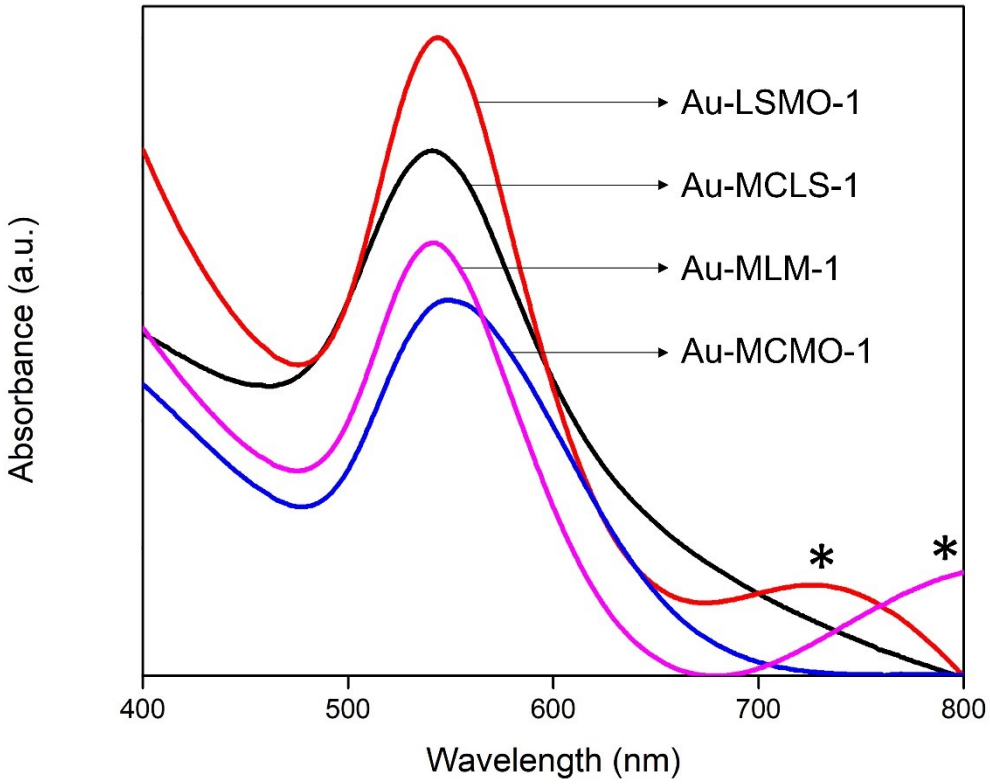

Figure S3 Absorbance spectra corresponding to biosynthesized Au nanoparticle systems: Au-MCLS-1 (541 nm), Au-LSMO-1 (543.75 nm and 730 nm), Au-MCMO-1 (548.75 nm), and Au-MLM-1 (541.75 nm and ~800 nm). Primary peaks are due to spherical or quasi-spherical nanoparticles, while secondary peaks* are attributed to nanoparticles with other shapes such as triangular, hexagonal plate-like, etc.

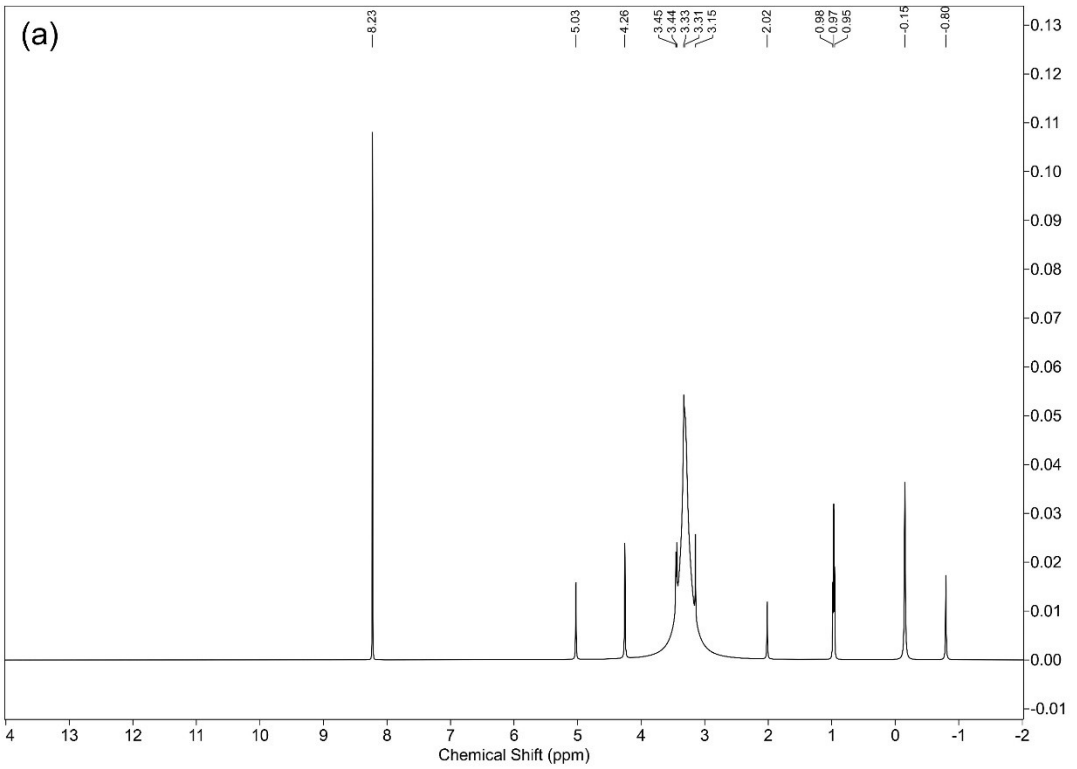
(a)
8.23
5.03
4.26
3.45
3.44
3.33
3.31
3.15
2.02
0.98
0.97
0.95
0.15
0.80
Chemical Shift (ppm)

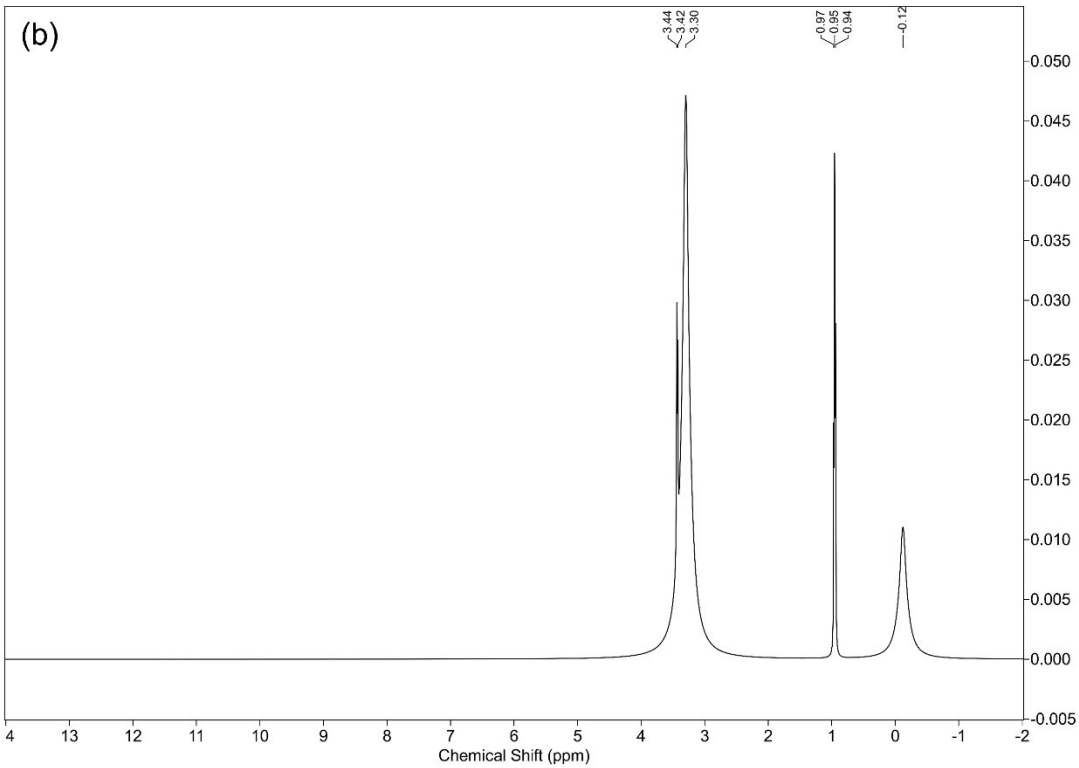
(b)
3.44
3.42
3.30
0.97
0.95
0.94
0.12
Chemical Shift (ppm)

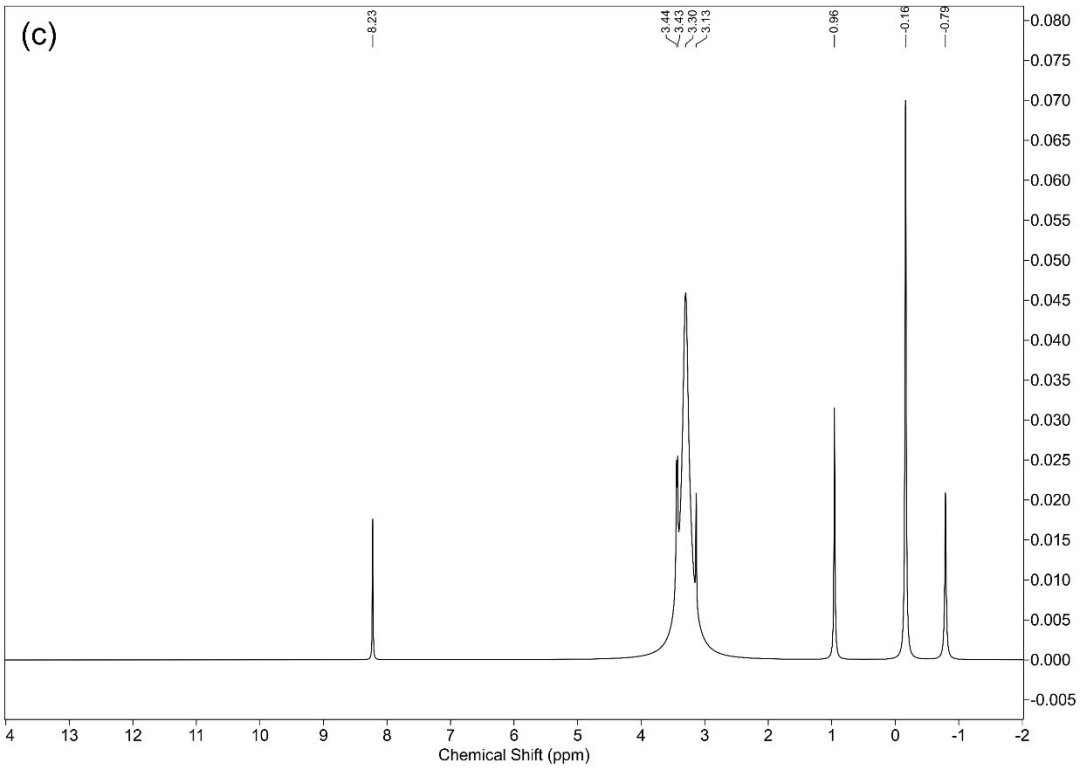

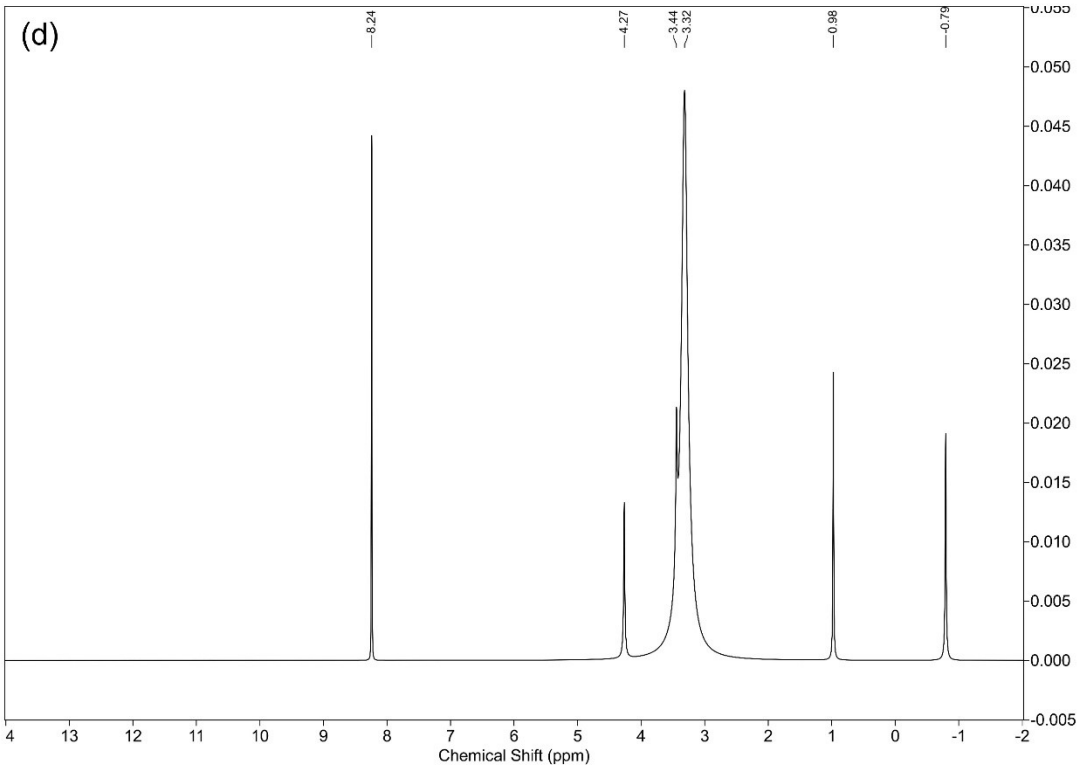

Figure S4 ^{1}H NMR (500 MHz, d_2o) analysis of the Au nanoparticle systems which were synthesized using different combinations of leaf extracts. (a) Au-MCLS-1 δ: -0.80, -0.15, 0.95, 0.97, 0.98, 2.02, 3.15, 3.31, 3.33, 3.44, 3.45, 4.26, 5.03, 8.23; (b) Au-LSMO-1 δ: -0.12, 0.94, 0.95, 0.97, 3.30, 3.42, 3.44; (c) Au-MCMO-1 δ: -0.79, -0.16, 0.96, 3.13, 3.30, 3.43, 3.44, 8.23, and (d) Au-MLM-1 δ: -0.79, 0.98, 3.32, 3.44, 4.27, 8.24.

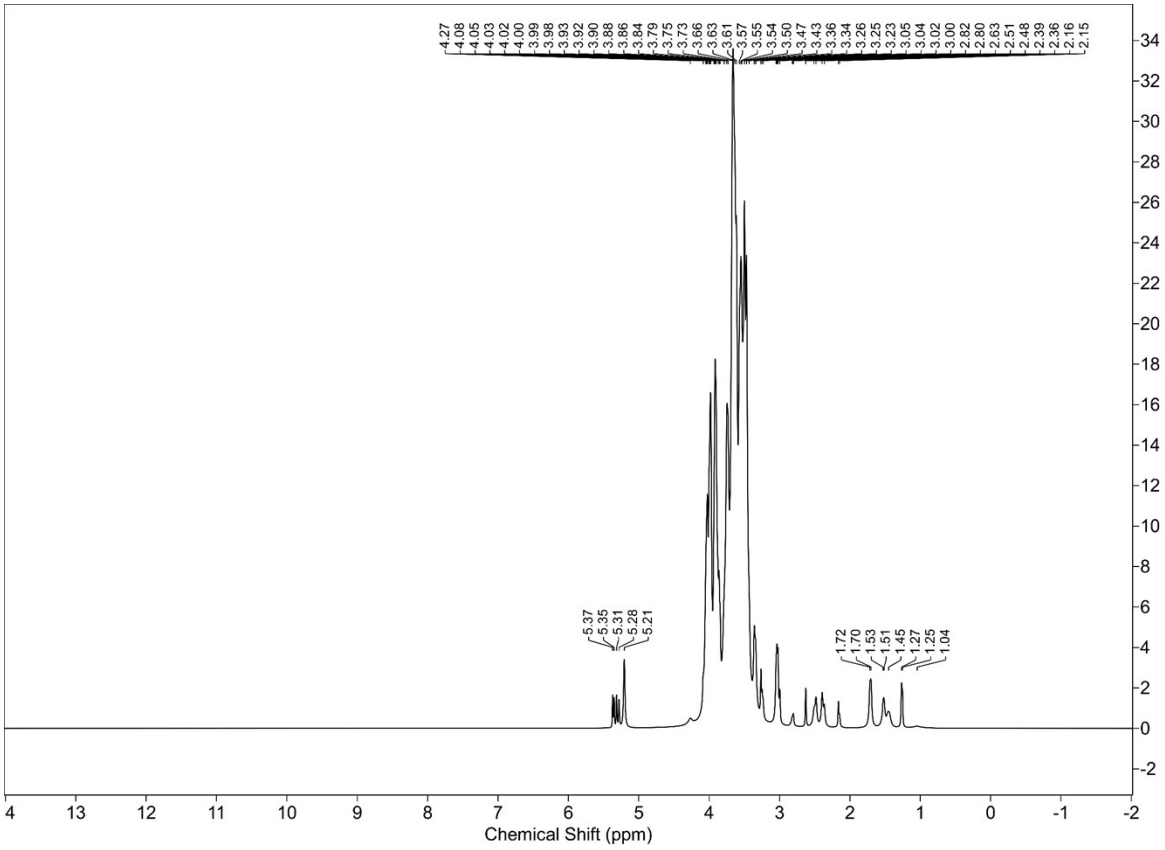

Figure S5 ^{1}H NMR (500 MHz, d_2o) analysis of Au-AS-1 δ: 1.04, 1.25, 1.27, 1.45, 1.51, 1.53, 1.70, 1.72, 2.15, 2.16, 2.36, 2.39, 2.48, 2.51, 2.63, 2.80, 2.82, 3.00, 3.02, 3.04, 3.05, 3.23, 3.25, 3.26, 3.34, 3.36, 3.43, 3.47, 3.50, 3.54, 3.55, 3.57, 3.61, 3.63, 3.66, 3.73, 3.75, 3.79, 3.84, 3.86, 3.88, 3.90, 3.92, 3.93, 3.98, 3.99, 4.00, 4.02, 4.03, 4.05, 4.08, 4.27, 5.21, 5.28, 5.31, 5.35, 5.37.

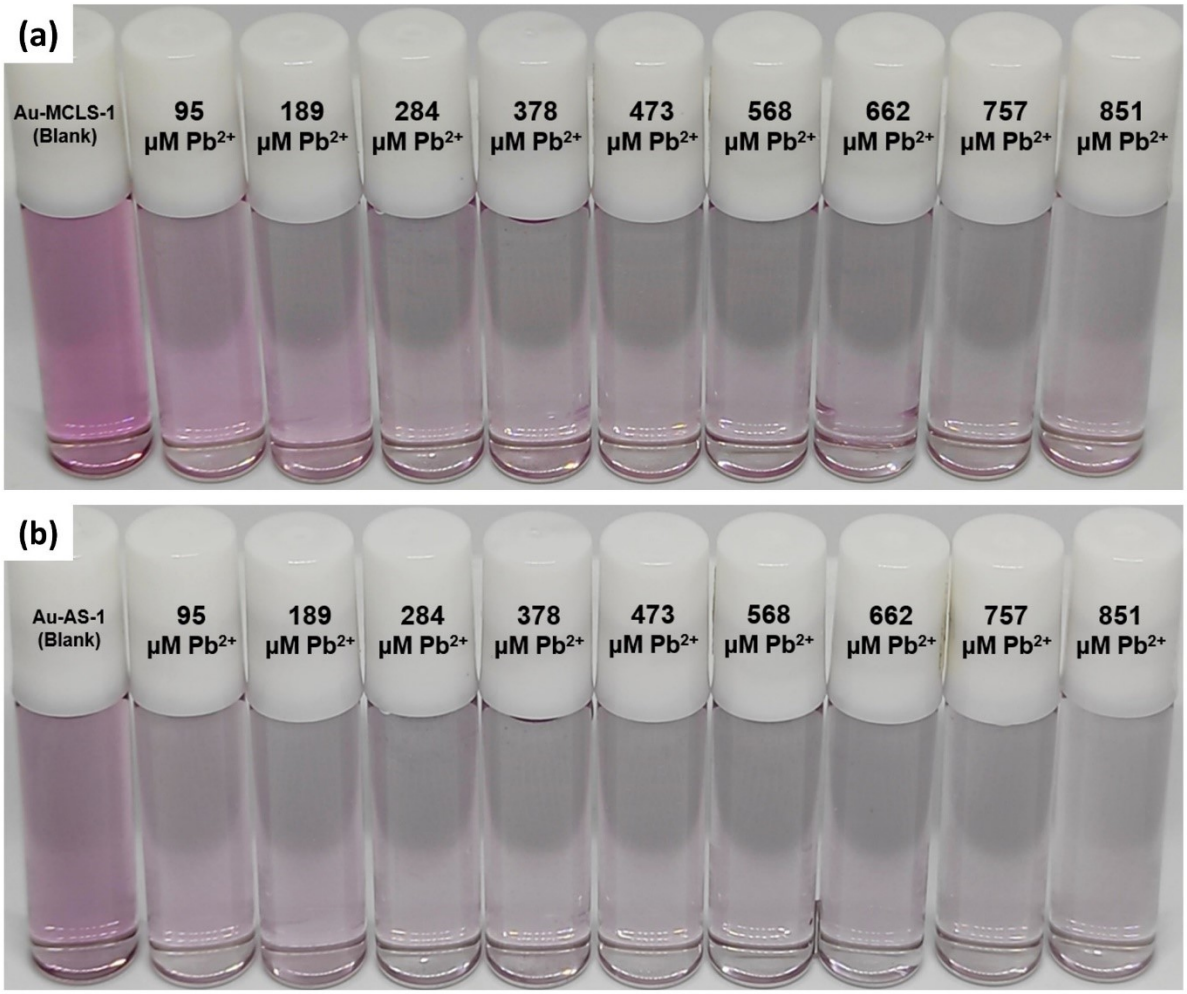

Figure S6 Comparison of (a) Au-MCLS-1 and (b) Au-AS-1 nanoparticle systems with varying Pb^{2+} concentrations showing solution color upon addition of lead ions.

Tables

Table S1 Combination Leaf Extracts

Combined Extracts	Extract Volume Ratio	Designated Sample Code
Muntingia calabura and *Lagerstroemia speciosa*	1:1	MCLS
Lagerstroemia speciosa and *Moringa oleifera*	1:1	LSMO
Muntingia calabura and *Moringa oleifera*	1:1	MCMO
Muntingia calabura, *Lagerstroemia speciosa* and *Moringa oleifera*	1:1:1	MLM

Participating Biochemical Compounds

The peaks of Au-MCLS-1 nanoparticles at 3834 and 3746 cm^{-1} correspond to the stretching of hydroxyl bonds from phenols which are isolated, free or non-hydrogen-bonded. These hydroxyl groups are the loose ends of the capping compounds of Au-MCLS-1 nanoparticles. Meanwhile, the 3475 cm^{-1} peak were attributed to the stretching of hydrogen-bonded hydroxyl groups which could be found at the capping compounds that interact with their neighboring hydrogen-bonding-capable structures. The hydrogen bond, which was considered strong, was represented by the peak at 2263 cm^{-1}. Moreover, the 2986 cm^{-1} peak was designated to alkane C-H stretching mode and the peak at 2350 cm^{-1} to the asymmetric stretching of the carbon dioxide molecule. Carbon dioxide molecules were adsorbed on the Au-MCLS-1 nanoparticles during air-drying prior to FTIR spectroscopy. The peaks at 2292 and 1537 cm^{-1} were assigned to N-H stretching and -NH deformation, respectively. The 1646 cm^{-1} peak was due to primary amide, while the peaks at 1725 and 1050 cm^{-1} were attributed to the carbonyl of carboxylic acid functional groups. Hydroxyl bending of phenols was associated with the peak at 1410 cm^{-1} and aromatic C-H out-of-plane bending was assigned to the 558 cm^{-1} peak.

Observed FTIR peaks of Au-LSMO-1 nanoparticles at 3851, 3734, and 3605 cm^{-1} were attributed to the stretching of phenolic hydroxyl groups which are free. These hydroxyl groups of the capping compounds were not hydrogen-bonded to their neighboring molecules. The peak at 3148 cm^{-1} was due to the N-H stretching, while the 2347 cm^{-1} peak was attributed to adsorbed carbon dioxide on the surface of Au-LSMO-1. The carbon dioxide molecules were adsorbed during the air-drying of nanoparticles. For the peaks at 1940 and 1831 cm^{-1}, the stretching modes of the carbonyl group were assigned. These carbonyl groups may be associated with original carbonyl structures of the polyphenols and organic acids or with hydroxyl groups which were reduced during the biosynthesis, and eventually acted as capping agents. In addition to these, carboxylic structures were ascribed to the peaks at 1725 and 1610 cm^{-1}. The peaks at 1194 and 1040 cm^{-1} may also be due to the carbon-oxygen bond of carboxylic acids. The N-H bond from secondary amide groups was designated to the peak at 1524 cm^{-1}, and the bending of C-H bond was assigned to the 1444 cm^{-1} peak. Moreover, the peak at 1347 cm^{-1} was due to the in-plane bending of primary or secondary hydroxyl groups and the 664 cm^{-1} peak was associated with the out-of-plane bending of OH. The peak at 759 cm^{-1} was attributed to the out-of-plane bending of aromatic C-H bond and the 496 cm^{-1} peak was due to the CC=O bending. For the weak band at 426 cm^{-1}, CCC deformations of phenyl ring (asymmetric bending) were ascribed.

Au-MCMO-1 nanoparticles generated FTIR peaks at 3848, 3719, 3658, and 3127 cm^{-1} which correspond to the stretching of hydroxyl groups which are free or isolated. These hydroxyl groups, attributed to polyphenols and organic acids, were on the surface of Au-MCMO-1 and not having significant hydrogen-bonding with their neighboring compounds. The carboxylic acid functional groups of the capping compounds were responsible for the peak at 1718 cm^{-1}. Meanwhile, the bending of the N-H bond in secondary amides was designated at the 1528 cm^{-1}

peak. The bending of CH_2 was attributed to the peak at 1429 cm^{-1} and the carbon-oxygen bond stretching which could be from carboxylic acids was ascribed to the peaks at 1203 and 1035 cm^{-1}. Moreover, the out-of-plane bending of hydroxyl groups corresponds to the 660 cm^{-1} peak, while the bending of CC=O was represented by the peak at 496 cm^{-1}. During the air-drying of Au-MCMO-1 nanoparticles, carbon dioxide molecules were also physisorbed on their surface as evidenced by the peak at 2345 cm^{-1}.

The FTIR peaks of Au-MLM-1 nanoparticles at 3851, 3735, and 3125 cm^{-1} were attributed to the stretching of hydroxyl groups. These hydroxyl groups were considered to be from the polyphenols that acted as capping compounds of the Au-MLM-1 nanoparticles. The peak at 1819 cm^{-1} corresponded to the stretching of the carbonyl group which could be from the original structure of polyphenols or organic acids, or could be due to the oxidation of some hydroxyl groups. Peaks at 1720 and 1600 cm^{-1} confirmed the presence of carboxylic structures of Au-MLM-1 capping compounds. Additional peaks at 1198 and 1057 cm^{-1} could also be attributed to the carbon-oxygen bond of carboxylic acids. Moreover, the peak at 1526 cm^{-1} was designated to be due to the amine functional group, while the bending of hydroxyl groups of phenolic structures is assigned to the 1327 cm^{-1} peak. The CCC out-of-plane bending was ascribed to the peak at 464 cm^{-1}. Au-MLM-1 nanoparticles also adsorbed carbon dioxide molecules during the drying process as signified by the 2350 cm^{-1} peak corresponding to the asymmetric stretching of carbon dioxide.

Table S2 Comparison of the Functional Groups of the Biosynthesized Au Nanoparticle Systems using Different Leaf Extract Combinations

Functional Group	**Au-MCLS-1**	**Au-LSMO-1**	**Au-MCMO-1**	**Au-MLM-1**
Free OH (polyphenols or organic acids)	Yes	Yes	Yes	Yes
H-bonded OH (polyphenols or organic acids)	Yes	No	No	No
-COOH (acidic compounds)	Yes	Yes	Yes	Yes
C=O	Yes	Yes	Yes	Yes
-NH (Amide I)	Yes	Yes	Yes	No
N-H (Amine)	No	Yes	No	Yes
C-H	Yes	Yes	Yes	No
CO_2 (adsorbed)	Yes	Yes	Yes	Yes

Table S3 Estimation of the Average Quasi-Spherical Au Nanoparticle Size and Polydispersity Index via Gaussian Fitting of Histograms from SEM Image Analysis

Au Nanoparticles	Number of Analyzed Particles	FWHM	Average Particle Diameter (nm)	Polydispersity Index
Au-MCLS-1	110	8.76	26 ± 4	0.021
Au-LSMO-1	47	14.97	37 ± 6	0.029
Au-MCMO-1	52	Peak 1: 9.44 Peak 2: 3.09	Peak 1: 14 ± 4 Peak 2: 24 ± 1 17 ± 6*	Peak 1: 0.077 Peak 2: 0.003 0.108*
Au-MLM-1	43	6.19	28 ± 3	0.009

*based on sample size data without Gaussian fitting

Note: The numbers of analyzed particles were dependent on the amount of particles with clear boundaries on the images.

Table S4 Summary of ^{1}H NMR Peak Commonality of Au-MCLS-1 and Au-AS-1 Nanoparticle Systems

1H NMR Spectral Range / Au NP System	8.23 Ar-H	5.37-5.21 Alliin, S-allylcysteine, Allicin, Ajoene	5.03 Alkene-H	4.27-4.26 H bonded to a cyclic structure or H bonded to C (bonded to another R group) of a cyclic structure	4.08-3.50 Alliin, S-allylcysteine, Allicin, Ajoene	3.45-3.44 H bonded to C (with OH) of a cyclic alcohol structure	3.43-3.34 Ajoene	3.33-3.31 Methoxy (O-CH3) or H bonded to C (with OH) of a cyclic alcohol structure	3.26-3.23 Alliin, S-allylcysteine	3.15 H bonded to C (with OH) of a cyclic alcohol structure or H bonded to a junction of cyclic structures	3.05-2.15 Alliin, S-allylcysteine, H-C-N and H-C-S from different compounds	2.02 H bonded to a junction of cyclic structures	1.72-1.04 Alkyl CH from different compounds	0.98 – -0.80 Methyl (R-CH3) Negative values: Due to aromatic ring-current effects
Au-MCLS-1	8.23		5.03	4.26		3.45 3.44		3.33 3.31		3.15		2.02		0.98 0.97 0.95 -0.15 -0.80
Au-AS-1		5.37 5.35 5.31 5.28 5.21		4.27 (extremely weak signal)	4.08 4.05 4.03 4.02 4.00 3.99 3.98 3.93 3.92 3.90 3.88 3.86 3.84 3.79 3.75 3.73 3.66 3.63 3.61 3.57 3.55 3.54 3.50 3.47		3.43 3.36 3.34		3.26 3.25 3.23		3.05 3.04 3.02 3.00 2.82 2.80 2.63 2.51 2.48 2.39 2.36 2.16 2.15		1.72 1.70 1.53 1.51 1.45 1.27 1.25 1.04	

Black regions indicate absence of peaks per Au nanoparticle system.

Table S5 Comparison of the Functional Groups of Au-MCLS-1 and Au-AS-1 Nanoparticle Systems

Functional Group	Au-MCLS-1	Au-AS-1
Free OH (polyphenols or organic acids)	Yes	Yes
Hydrogen-bonded OH (polyphenols or organic acids)	Yes	No
Alkane C-H	Yes	No
-COOH (acidic compounds)	Yes	No
Aromatic C-H (phenolic compounds)	Yes	No
-NH (primary amide)	Yes	Yes
-NH (alliin, S-allylcysteine)	No	Yes
OH (carboxylic acid: alliin, S-allylcysteine)	No	Yes
Alkenyl C=C (alliin, S-allylcysteine, allicin, ajoene)	No	Yes
C=O (carboxylic acid: alliin, S-allylcysteine)	No	Yes
C-N (amines: alliin, S-allylcysteine)	No	Yes
S=O (alliin, allicin, ajoene)	No	Yes
Alkene C-H (alliin, S-allylcysteine, allicin, ajoene)	No	Yes
C-S (alliin, S-allylcysteine, allicin, ajoene)	No	Yes
S-S (allicin, ajoene)	No	Yes
CO_2 (adsorbed)	Yes	Yes

LSPR Peak FWHM Behavior with Varying Ion Concentrations

The full width at half maximum (FWHM) of the absorbance spectra of Au-MCLS-1 with varying Pb^{2+} exhibited almost similar trend with the plot of LSPR peak shift (nm) versus concentration (μM). The linearly increasing region where LSPR peak broadening was observed before the fluctuations occurred could imply formation of larger and more polydispersed particle aggregates. The effects of Pb^{2+} or Zn^{2+} to the FWHM of Au-MCLS-1 absorbance spectra are in agreement with the observed LSPR peak shifts and suppression. Both ions were able to broaden the LSPR peak of Au-MCLS-1 wherein Pb^{2+} has more pronounced effect as compared to Zn^{2+}. Since Pb^{2+} species were able to induce larger peak shift, suppression, and broadening, Au-MCLS-1 could have weaker attractive forces with Zn^{2+}.

Moreover, the measured FWHM values of the absorbance spectra of Au-AS-1 with varying Pb^{2+} showed some fluctuations with an apparent generally increasing trend. This general LSPR peak broadening trend as Pb^{2+} concentration increases could be attributed to the agglomeration of nanoparticles as the ions increase interparticle attractions.

One parameter which could verify the selectivity of Au-AS-1 nanoparticle system is the FWHM of the absorbance spectra. Increasing FWHM or broadening of the LSPR peak could be associated with the nanoparticles moving closer to one another due to ion-induced attractive forces. For Au-AS-1 nanoparticles, a significant increase in the measured FWHM was only observed upon the exposure to Pb^{2+}, but not with Zn^{2+}. An interpretation of this is that Au-AS-1 nanoparticles do not have significant attractive interactions with Zn^{2+}, hence is more selective to Pb^{2+}. Due to this observed selectivity, Au-AS-1 nanoparticle system has potential in the detection of Pb^{2+} even if Zn^{2+} are both in the analyte.